Research Notes: Tabak-Rinzel, eupnea, sigh, and calcium dynamics

Greg Conradi Smith, Daniel Scott Borrus, Christopher Del Negro

January 19, 2021

1 Construction a Model of the Eupnea and Sigh Rhythms

1.1 An Activity Model of Episodic Bursting

We model the eupnea subsystem in a manner similar to Tabak and Rinzel (**?**). In the original Tabak-Rinzel model, the ODE representing network activity (firing rate) takes the form $\tau_a da/dt = a_\infty(w \cdot s \cdot d \cdot a) - a$ where s and d represent synaptic depression operating on a slow and fast time scales.

The steady state activity is the following sigmoidal function of synaptic input (x): $a_\infty(x) = [1 + e^{4(\theta_a - x)/k_a}]^{-1}$.

Fast synaptic depression leads to oscillatory dynamics during the active phase of each burst. These oscillations do not occur in our case, so the ODEs that are our starting point are $\tau_a da/dt = a_\infty(w \cdot s \cdot a) - a$ and $\tau_s ds/dt = s_\infty(a) - s$ where the steady state activity (firing rate) is the following sigmoidal function of synaptic input (x): $a_\infty(x) = [1 + e^{4(\theta_a - x)/k_a}]^{-1}$. Similarly, the steady state synaptic depression is a sigmoidal function of network activity: $s_\infty(a) = [1 + e^{4(\theta_s - a)/k_s}]^{-1}$. Thus, our two state variables can be written

$$\tau_a \frac{da}{dt} = a_\infty(w \cdot s \cdot a) - a \tag{1}$$

$$\tau_s \frac{ds}{dt} = s_\infty(a) - s \tag{2}$$

where a is the network activity and s accounts for the dynamics of synaptic depression. Note that when $s = 0$, the system is fully depressed. The steady state functions a_∞ and s_∞ are given by

$$a_\infty(x) = \frac{1}{1 + e^{4(\theta_a - x)/k_a}} \tag{3}$$

$$s_\infty(x) = \frac{1}{1 + e^{4(\theta_s - x)/k_s}} \tag{4}$$

Note: When k_a is positive (negative), a_∞ is a monotone decreasing (increasing) function of x, and similarly for k_s/s_∞. The 4 that appears in Eqs. 3 and 4 makes k_a and k_s the inverse of the slope of a_∞ and s_∞ at the half-max.

Fig. 1 shows that depending on the strength (gain) of recurrent excitation, denoted by w, the network activity can have 1–3 steady states. For intermediate values of w the excitatory network is bistable.

The a and s nullclines are given by $a = a_\infty(w \cdot s \cdot a)$ and $s = s_\infty(a)$. The first expression is implicit, but it can be written explicitly by viewing s as a function of a:

$$a \text{ nullcline:} \quad a = a_\infty(w \cdot s \cdot a) \Longrightarrow s = \frac{4\theta_a - k_a \ln\left[(1-a)/a\right]}{4wa} \,.$$

The system can be configured into two unique forms of excitability, depending on the parameters used. Fig. 2 shows the nullclines of two distinct parameter sets corresponding to type 2 (left) and type 1 (right) excitability. In type 2 excitability, oscillations occur as a result of a super-critical hopf bifurcation. In type 1 excitability, oscillations arise from a saddle-node on an invariant circle, or SNIC, bifurcation.

As we adapt this model to represent a population of firing neurons, it will be helpful to assign realistic units to the firing rate, a. Rather than a representing the fraction of firing cells, we assign a units of spikes per neuron per second. When this is the case, a can be greater than 1, however the behavior of the a nullcline doesn't change that much. When $\lim_{x\to\infty} a_\infty(x) = a_{max} \neq 1$, the equation for the a nullcline is

$$a \text{ nullcline:} \quad a = a_\infty(w \cdot s \cdot a) \Longrightarrow s = \frac{4\theta_a - k_a \ln\left[(a_{max}-a)/a\right]}{4wa} \,.$$

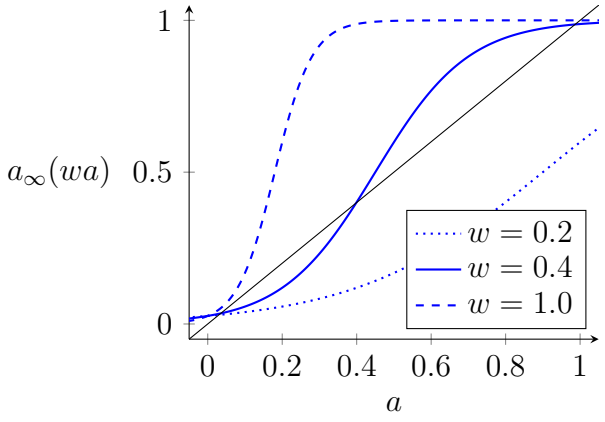

Figure 1: For intermediate values of w the excitatory network is bistable. Synaptic depression is off ($s = 1$). Parameters: $\theta_a = 0.18$, $k_a = 0.2$

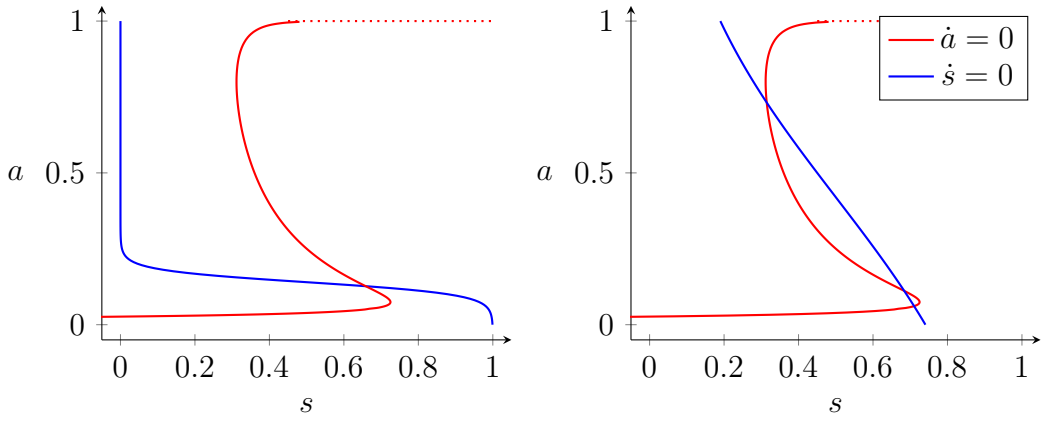

Figure 2: Nullcines for the modified Tabak-Rinzel model. Left: Type 2 oscillations; $\theta_s = 0.14$, $k_s = -0.08$. Right: Type 1 excitability; $\theta_s = 0.42$, $k_s = -1.6$. Other parameters: $w = 1$, $\tau_a = 10$, $\theta_a = 0.18$, $k_a = 0.2$.

1.2 Introducing Membrane Noise

So far we have assumed deterministic dynamics. Intrinsic stochastic dynamics of the excitatory network is modeled by additive Gaussian white noise with state-dependent variance to Eq. 1. The model is now written

$$\tau_a \frac{da}{dt} = a_\infty(w \cdot s \cdot a) - a + \hat{\xi}_a(a(t)) \quad (5)$$

$$\tau_s \frac{ds}{dt} = s_\infty(a) - s \quad (6)$$

The noise term has mean zero, i.e., $\langle \hat{\xi}_a \rangle = 0$. The variance of the Gaussian white noise is derived by considering the rates of the forward and reverse elementary processes implied by the deterministic ODE for the network activity. Consider the deterministic part of Eq. 1:

$$\frac{da}{dt} = \frac{a_\infty(wa) - a}{\tau_a}$$

where we note that $\lim_{x \to -\infty} a_\infty(x) = 0$ and write a_{max} for the limit of $a_\infty(x)$ as $x \to \infty$. Defining

$$\tau_a = \frac{1}{\alpha + \beta} \quad \text{and} \quad a_\infty = \frac{\alpha}{\alpha + \beta} a_{max}$$

we have

$$\alpha = \frac{a_\infty}{a_{max}\tau_a} \quad \text{and} \quad \beta = \frac{a_{max} - a_\infty}{a_{max}\tau_a}$$

Thus Eq. 1 can be written as

$$\frac{da}{dt} = \alpha(a_{max} - a) - \beta a$$

This is consistent with the elementary processes shown in this diagram:

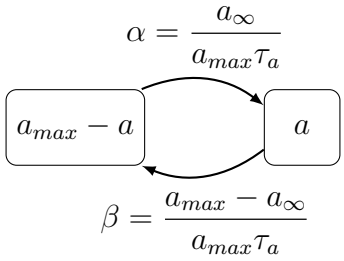

This leads to the following expression for the two-time covariance

$$\langle \hat{\xi}_a(t) \hat{\xi}_a(t') \rangle = \gamma_a(a, s)\delta(t - t')$$

where

$$\gamma_a(a, s) = \frac{1}{N}\left[\alpha \cdot (a_{max} - a) + \beta \cdot a\right] = \frac{1}{N a_{max}\tau_a}\left[a_\infty \cdot (a_{max} - a) + (a_{max} - a_\infty)a\right] \quad (7)$$

Figure 3 describes the size of the fluctuations as a function of the activity level.

$[a_\infty \cdot (a_{max} - a) + (a_{max} - a_\infty)a]$

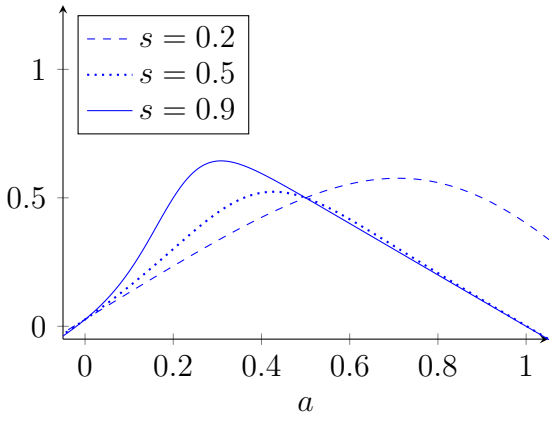

Figure 3: Size of fluctuations as given by Eq. 7. The size of the noise depends on the network firing rate a and synaptic depression s. Other parameters are the default values: $\theta_a = 0.18$, $k_a = 0.2$, $w = 1$.

1.3 System Limitations Arising from One Slow Variable

How well does our simulation of the preBötC inspiratory rhythm emulate the *in vitro* recordings? Figure 4A shows a canonical *in vitro* network field recording of preBötC electrical activity. Focus on two important characteristics of this rhythm, encapsulated by the scatter and histogram plots on the right. First, the size of a burst event has no relationship with the duration of the preceding interval. This neutral correlation is depicted in the scatter plot of Figure 4. Second, the distribution of inter-event intervals appears normally distributed, as shown in the histogram, which is simply a flattening of the scatter plot along the x-axis.

Reviewing the model, Figure 4B depicts the trajectories of a and s when the system is configured for type 2 excitability. Here, the oscillations arise from a supercritical-hopf bifurcation (HB), and the appearance of a stable limit cycle. (should we include the bif. diagram?) The timing between each burst event is normally distributed, just like it is in the biology. The events are normal distributed because membrane noise either increases or decreases the total time synaptic depression can recover. However, this will lead to a problem with burst size.

Take another look at the nulc lines in Figure 4B. We can see the membrane noise manifesting in the system at the bottom knee of the a nullcline. Each burst has a slight variation in when it falls off this knee, which leads to variation of the peak amplitude of the synaptic depression. This proves to be critical to the behavior of the system. If a burst is delayed, then the synaptic depression term recovers to a greater degree, and the ensuing burst will be larger. The reverse is true for bursts with short preceding intervals. Ultimately, this leads to a positive correlation between preceding interval and burst size, as depicted in the scatter plot of Figure 4B.

Figure 4C depicts the system in type-1 excitability. Here the system is subcritical to a saddle-node on an invariant circle (SNIC) bifurcation. Now the synaptic depression recovers to a maximum value before every burst. The burst size is no longer dependent on the duration of the preceding inter-event interval. Because the system is subcritical, it will not fire without some sort of noise. Membrane noise drives the system over the threshold, and triggers an event. Herein lies another problem.

The membrane noise is driven by a Wiener process. As we wait for the noise to integrate above some threshold, we are waiting for a random event with some known probability to occur. This describes a Poisson process, and the timing between successive events will therefore follow an exponential distribution. Indeed, in the model with a type-1 configuration, the timing between burst events appears to be exponentially distributed (after some minimal time, corresponding to synaptic depression recovery). We know breaths are not exponentially distributed *in vivo*. That would be a terrifying phenomenon. We also know breathes are not exponentially distributed *in vitro* (Figure 4A).

Thus we are at an impasse with our two variable model. In the type-2 configuration, the timing between the events is normally distributed, but there is an unrealistic relationship between the size of the burst events and the duration of the preceding interval. In the type-1 configuration, similar to the biology, there is no relationship between burst size and the preceding interval. However, here the timing between the events is exponentially distributed, which does not represent the biology either. From here, in order to bring our model into

agreement with what we observe physiologically, we reason we needed an additional slow variable.

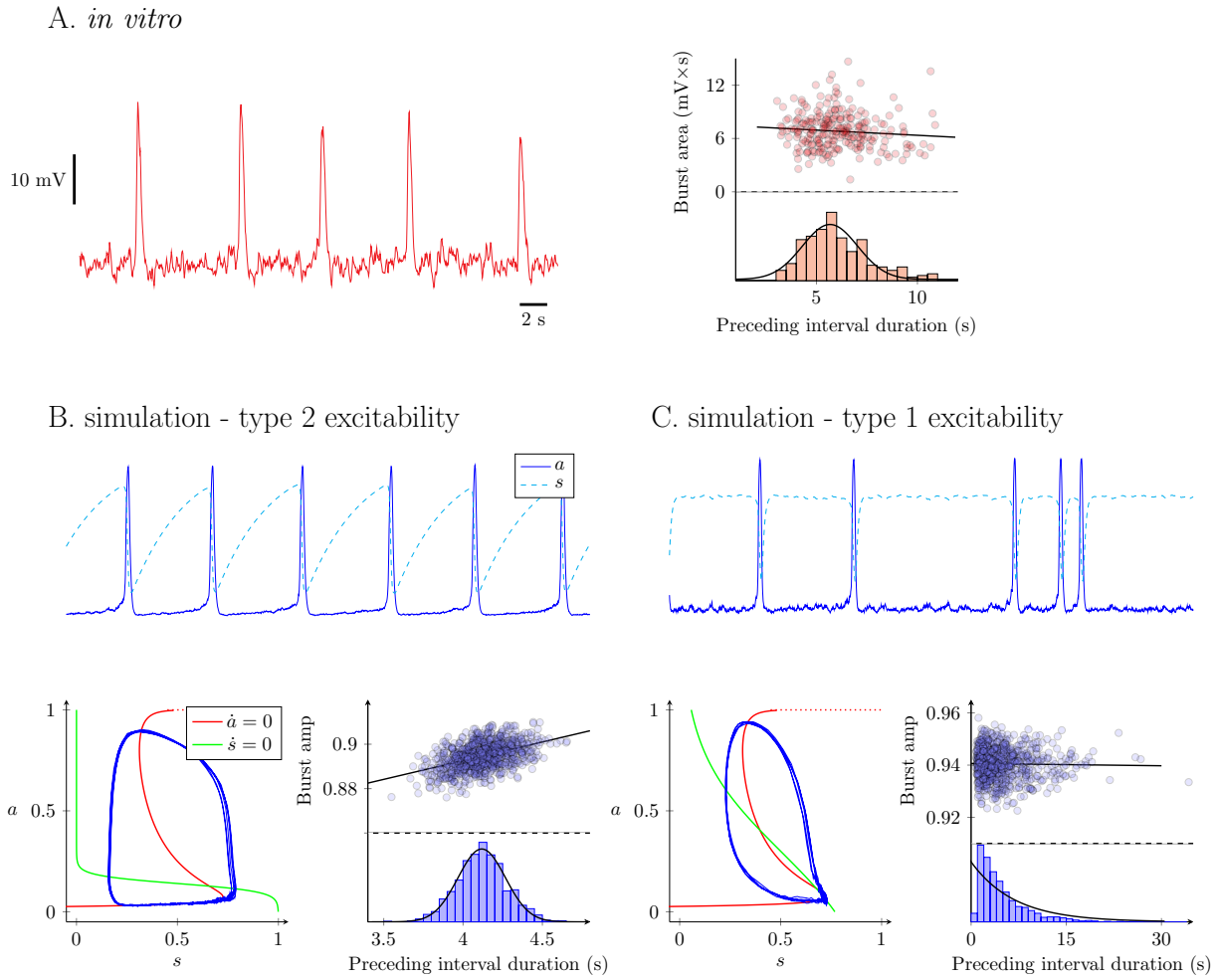

Figure 4: Limitations of only two slow variables in the eupnea model. **A.** network recording of preBötC activity. Right: a scatter plot describing the relationship between the duration of the preceding event interval and the size (area) of the subsequent network burst. Below the scatter plot is a histogram describing the distribution of inter-event intervals. Note the histogram is a flattening of the scatter plot down onto the x-axis. **B.** 2-state model in a type-2 configuration. Shown is one solution and the phase space with nulclines. A scatter plot describing burst amplitude with preceding interval is also shown, with a histogram describing the inter-event interval distribution. **C.** the model in type 1 excitability configuration.

1.4 The Eupnea Subsystem

We model the eupnea subsystem using the following modifications of the Tabak-Rinzel-like model presented in the previous sections. However, here we include both synaptic depression (s) and cellular adaptation (θ). The ODEs for our modification of the Tabak-Rinzel model are

$$\tau_a \frac{da}{dt} = a_\infty(w \cdot s \cdot a - \theta) - a + \hat{\xi}_a(a(t)) \tag{8}$$

$$\tau_s \frac{ds}{dt} = s_\infty(a) - s \tag{9}$$

$$\tau_\theta(a) \frac{d\theta}{dt} = \theta_\infty(a) - \theta \tag{10}$$

where the variable θ is an adaptive threshold for the activity as a function of synaptic input. The steady state functions a_∞ and s_∞ are given by Eqs. 3 and 4. The steady-state function θ_∞ is analogous:

$$\theta_\infty(x) = \frac{1}{1 + e^{4(\theta_\theta - x)/k_\theta}} \,. \tag{11}$$

The dependence of τ_θ on the activity level is chosen to be

$$\tau_\theta(x) = \frac{\tau_\theta^{max} - \tau_\theta^{min}}{1 + e^{4(\theta_{\tau_\theta} - x)/k_{\tau_\theta}}} + \tau_\theta^{min} \,. \tag{12}$$

This is important because the cellular adaptation needs to happen quickly in the active phase (when a is large), but recover slowly during the silent phase (when a is small). Figure 5 demonstrates the three state system undergoing oscillations. Synaptic depression terminates the bursts, and the recovery of the adaptation variable (θ) determines the timing of the subsequent burst.

This model for eupnea generation is inline with what we observe biologically. The timing between the burst events is normally distributed, and there is no significant relationship between the duraiton of the preceding interval and the size of the subsequent burst (Figure 5).

Table 1 describes the default parameters used for the eupnea subsystem.

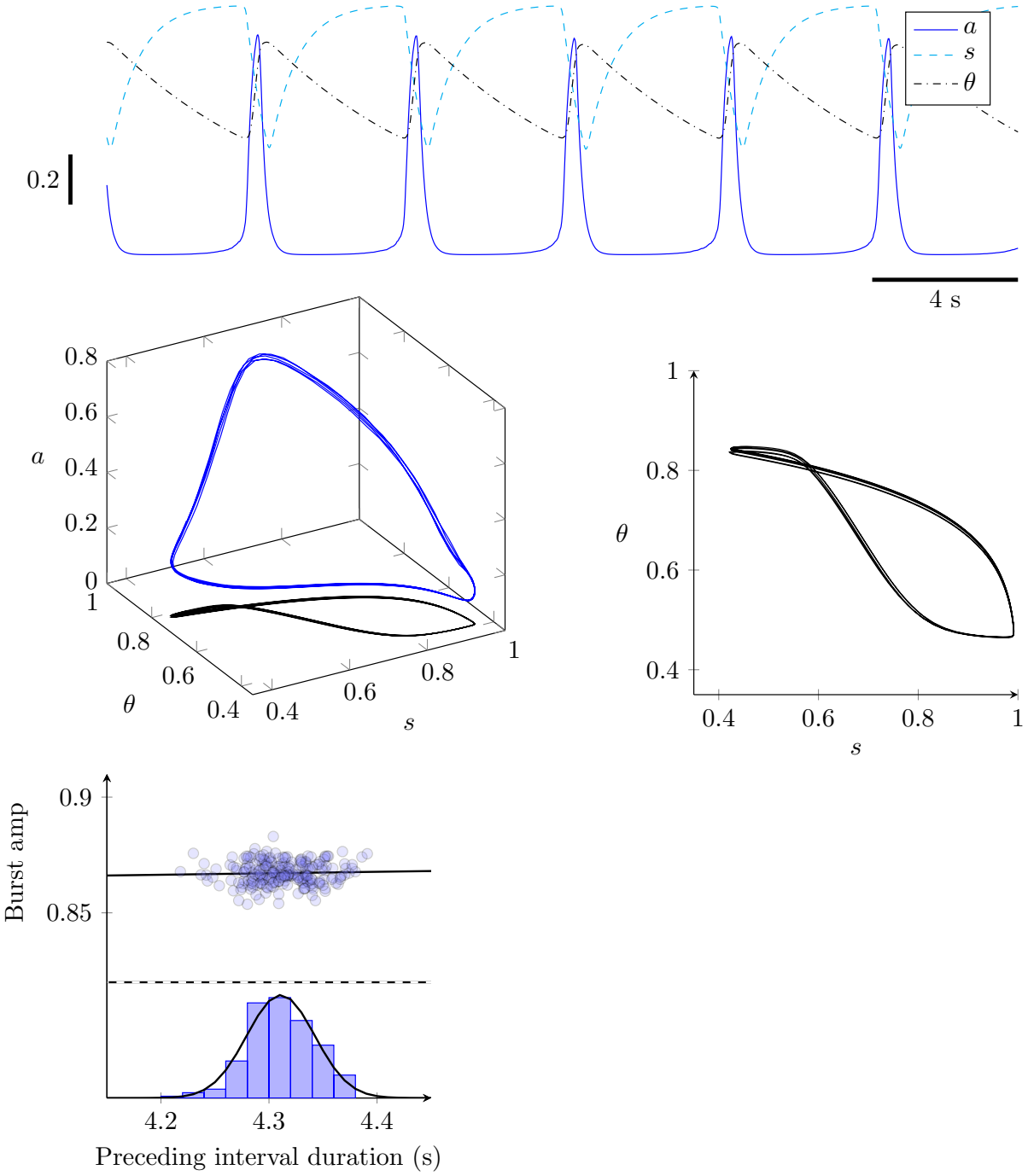

Figure 5: Tabak-Rinzel like model with two slow variables (s and θ). Top trace shows the trajectory of the three-state model. The middle left plot shows this solution in a 3-dimensional phase space. The middle right plot focuses on the relationship between cellular adaption (θ) and synaptic depression (s). The bottom graph contains a scatter plot describing the relationship between preceding intervals with burst size. The scatter plot is condensed into a histogram to show the event intervals are normally distributed.

Symbol	Definition	Value	Units
w	network connectivity	1	-
θ_a	average firing threshold (half activation)	$[-0.3, 0.1]$	
k_a	reciprocal of slope of a_∞ at half activation	2	
τ_a	network recruitment time constant	0.15	
θ_s	half activation of s	0.14	
k_s	reciprocal of slope of s_∞ at half activation	-0.08	
τ_s	time constant of synaptic depression	0.75	
θ_θ	half activation of θ	1.5	
k_θ	reciprocal of slope of θ_∞ at half activation	2	
τ_θ^{max}	maximum of time constant of cellular adaptation	6	
τ_θ^{min}	minimum of time constant of cellular adaptation	0.15	
θ_{τ_θ}	half max of $\tau_\theta(a)$	3	
k_{τ_θ}	reciprocal of slope of $\tau_\theta(a)$ at half activation	5	

Table 1: Description of parameters for eupnea model and standard values.

The sigh model: calcium handling

Closed cell Ca^{2+} model with bistability

We propose the sigh rhythm emerges from intracellular Ca^{2+} dynamics. We borrow the template for modeling Ca^{2+} handling from Keizer and Levine 1996. Our description of the equations begins with a closed system, where the total calcium in the cell is fixed and calcium moves between the cytosol and intracellular Ca^{2+} stores, such as the ER.

$$\frac{dc}{dt} = [v_1 r_\infty(c) + v_2]\,(c_{er} - c) - \frac{v_3 c^2}{k_3^2 + c^2} \tag{13}$$

$$c_{er} = (c_{tot} - c)/\lambda \tag{14}$$

Breaking this ODE down, the terms $v_1 r_\infty(c)$ describe Ca^{2+} leaving the ER via Ca^{2+}-induced-Ca^{2+}-release. This process is mediated, in theory, by IP3 receptors and ryanodine receptors on the ER and other calcium sequestering organelles. The variable v_2 describes the passive Ca^{2+} leak from the ER to the cytosol. Both of these processes are proportional to a driving force, $(c_{er} - c)$. Lastly, the variable v_3 controls the rate of Ca^{2+} in the cytosol being pumped into the ER via SERCA pumps on the walls of the ER.

Because Ca^{2+} cannot leave the cell in this model, the total calcium is fixed, and can be calculated.

$$c_{tot} = \lambda c_{er} + c \tag{15}$$

λ is a scaling factor for the ER to account for a large change in volume compared to the cytosol; this parameter keeps concentration in both chambers consistent.

The phase diagram for Eq. 13 is shown in Figure 6. Depending on the total calcium in the cell, there are 1–3 steady states for the Ca^{2+} subsystem.

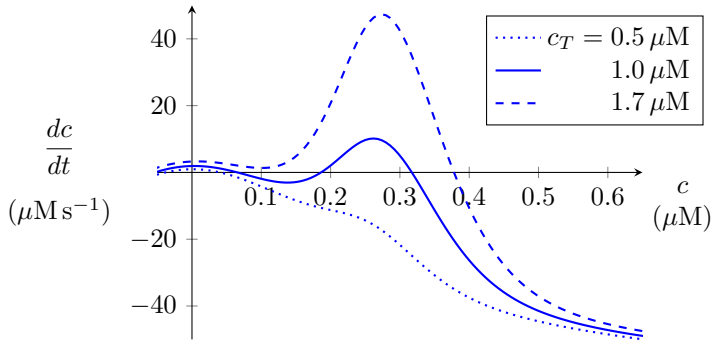

Figure 6: Closed cell model. Parameters: $\theta_m = 0.25$, $k_m = 0.04$, $\theta_h = 0.3$, $k_h = -0.06$, $\lambda = 0.15$, $v_1 = 40$, $v_2 = 0.5$, $v_3 = 120$, $k_3 = 0.3$.

Open cell Ca^{2+} model

Eqs. 13 and 14 can be modified to allow for Ca^{2+} fluxes across the plasma membrane. See the changes in Eq. 16. The total Ca^{2+} concentration in the cell (c_{tot}) is no longer fixed. $\jmath_0$ controls the Ca^{2+} flux into the cytosol from outside the cell. v_4 regulates the rate Ca^{2+} is pumped out of the cell.

$$\frac{dc}{dt} = [v_1 f_\infty(c) + v_2]\,[c_{er} - c] - \frac{v_3 c^2}{\kappa_3^2 + c^2} + \jmath_0 - \frac{v_4 c^4}{\kappa_4^4 + c^4} \tag{16}$$

$$\frac{dc_{tot}}{dt} = \jmath_0 - \frac{v_4 c^4}{\kappa_4^4 + c^4} \tag{17}$$

where $c_{er} = (c_{tot} - c)/\lambda$ and

$$f_\infty(c) = \frac{1}{1 + e^{(\theta_m - c)/k_m}} \cdot \frac{1}{1 + e^{(\theta_h - c)/k_h}}$$

where $k_m > 0$ and $k_h < 0$. $f_\infty(c)$ still describes the rate of Ca^{2+}-induced-Ca^{2+}-release and takes the form of a bell shaped curve.

The dynamics of the open cell Ca^{2+} subsystem are described in Figure 7. Default parameters are written in Table 2.

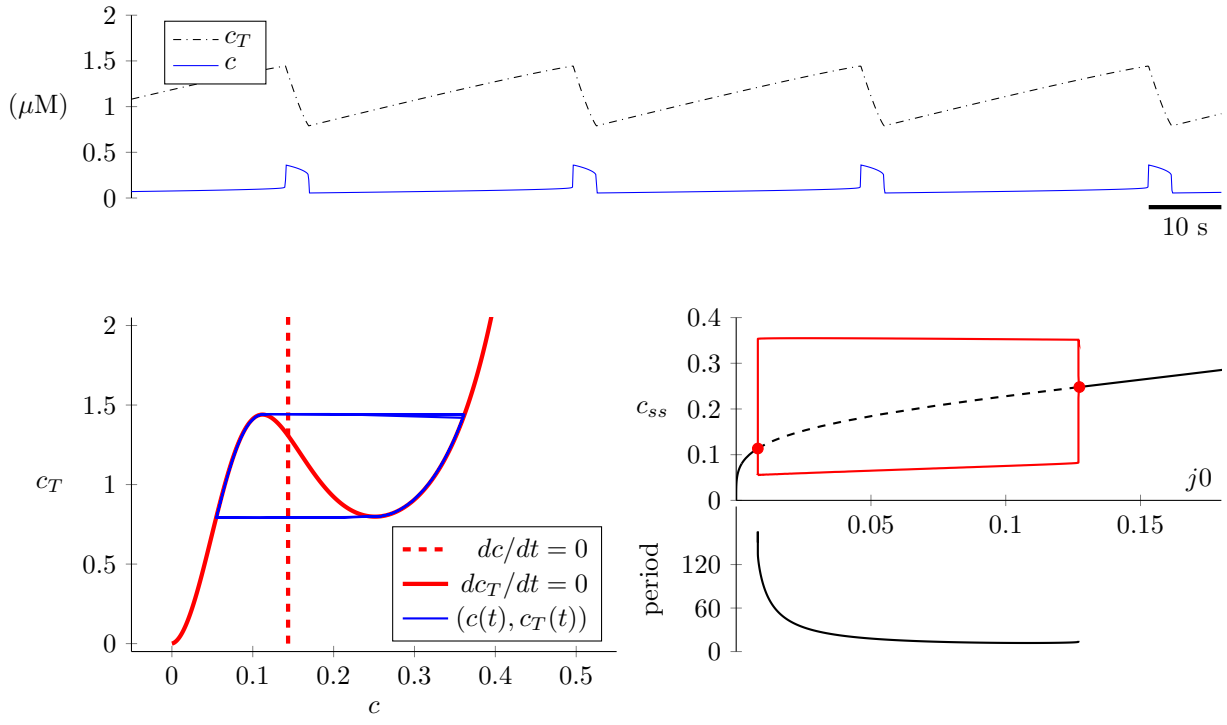

Figure 7: Open cell calcium dynamics. Calcium subsystem only.

Symbol	Definition	Value	Units
v_1	rate constant of calcium release	20	s^{-1}
v_2	rate constant of calcium leak	0.25	s^{-1}
v_3	maximum rate of SERCA pumps	60	$\mu\mathrm{M}\,\mathrm{s}^{-1}$
k_3	half maximum for SERCA pumps	0.3	$\mu\mathrm{M}$
n_3	Hill coefficient for SERCA pumps	2	-
λ	ER/cytosol effective volume ratio	0.15	-
θ_m	activation of intracellular calcium channels	0.25	$\mu\mathrm{M}$
k_m	reciprocal of slope of m_∞ at half maximum	0.04	-
θ_h	activation of intracellular calcium channels	0.3	$\mu\mathrm{M}$
k_h	reciprocal of slope of h_∞ at half maximum	-0.06	-
j_{in}^0	constant calcium influx rate	0.009	$\mu\mathrm{M}\,\mathrm{s}^{-1}$
j_{in}^1	calcium influx rate proportionality constant	0.02	$\mu\mathrm{M}\,\mathrm{s}^{-1}/activity$
v_4	maximum rate of PMCA pumps	0.4	$\mu\mathrm{M}\,\mathrm{s}^{-1}$
k_4	half maximum for PMCA pumps	0.3	$\mu\mathrm{M}$
n_4	Hill coefficient for PMCA pumps	4	-

Table 2: Description of parameters for calcium handling and standard values.

The Tabak-Rinzel-like activity model with calcium dynamics

We connect the eupnea and calcium subsystems to model the eupnea and sigh rhythms in the preBötC.

$$\begin{aligned}
\tau_a \frac{da}{dt} &= a_\infty(w \cdot s \cdot a - \theta, c) - a + \hat{\xi}(a) \\
\tau_s \frac{ds}{dt} &= s_\infty(a) - s \\
\tau_\theta(a) \frac{d\theta}{dt} &= \theta_\infty(a) - \theta \\
\frac{dc}{dt} &= [v_1 f_\infty(c) + v_2]\,[c_{er} - c] - \frac{v_3 c^2}{\kappa_3^2 + c^2} + \jmath_0 + \jmath_1 a - \frac{v_4 c^4}{\kappa_4^4 + c^4} \\
\frac{dc_{tot}}{dt} &= \jmath_0 + \jmath_1 a - \frac{v_4 c^4}{\kappa_4^4 + c^4}
\end{aligned}$$

where $c_{er} = (c_{tot} - c)/\lambda$ and

$$f_\infty(c) = \frac{1}{1 + e^{(\theta_m - c)/k_m}} \cdot \frac{1}{1 + e^{(\theta_h - c)/k_h}}$$

where $k_m > 0$ and $k_h < 0$. We assume that the steady state function a_∞ is 'boosted' by the intracellular calcium concentration, as follows:

$$a_\infty(x, c) = \frac{\lambda_a}{1 + e^{4(\theta_a - x)/k_a}} + \frac{\lambda_c}{1 + e^{4(\theta_c - c)/k_c}}$$

where λ_c is the contribution of intracellular Ca^{2+} to network activity. This is comparable to activation of a Ca^{2+}-activated Na^+ current (I_{CAN}). Activity is tied back into the Ca^{2+} subsystem via the $\jmath_1$ term. When activity in the network is high, Ca^{2+} enters the cytosol at a rate proportional to $\jmath_1$. These terms are responsible for welding the two subsystems together.

The steady state cytosolic calcium concentration solves the implicit expression

$$0 = (v_1 + v_2 r_\infty(c)) \left(\frac{c_{tot} - c}{\lambda} - c \right) - \frac{v_3 c^2}{\kappa^2 + c^2} + \jmath_0 + \jmath_1 a - \frac{v_4 c^4}{\kappa_4^4 + c^4},$$

but this can be written as an explicit expression for c_{tot} as a function of c,

$$c_{tot} = (\lambda + 1)c - \frac{\lambda}{v_1 + v_2 r_\infty(c)} \left(-\frac{v_3 c^2}{\kappa^2 + c^2} + \jmath_0 + \jmath_1 a - \frac{v_4 c^4}{\kappa_4^4 + c^4} \right)$$

. The steady state total calcium concentration can also be calculated.

$$\begin{aligned}
0 &= \jmath_0 + \jmath_1 a - \frac{v_4 c^4}{\kappa_4^4 + c^4} \\
c &= \left(\frac{\kappa_4^4 (\jmath_0 + \jmath_1 a)}{v_4 - \jmath_0 + \jmath_1 a} \right)^{1/4}
\end{aligned}$$

Trajectories of the entire system are shown in Figure 8. The faster eupnea oscillation and the slower sigh oscillation run in parallel.

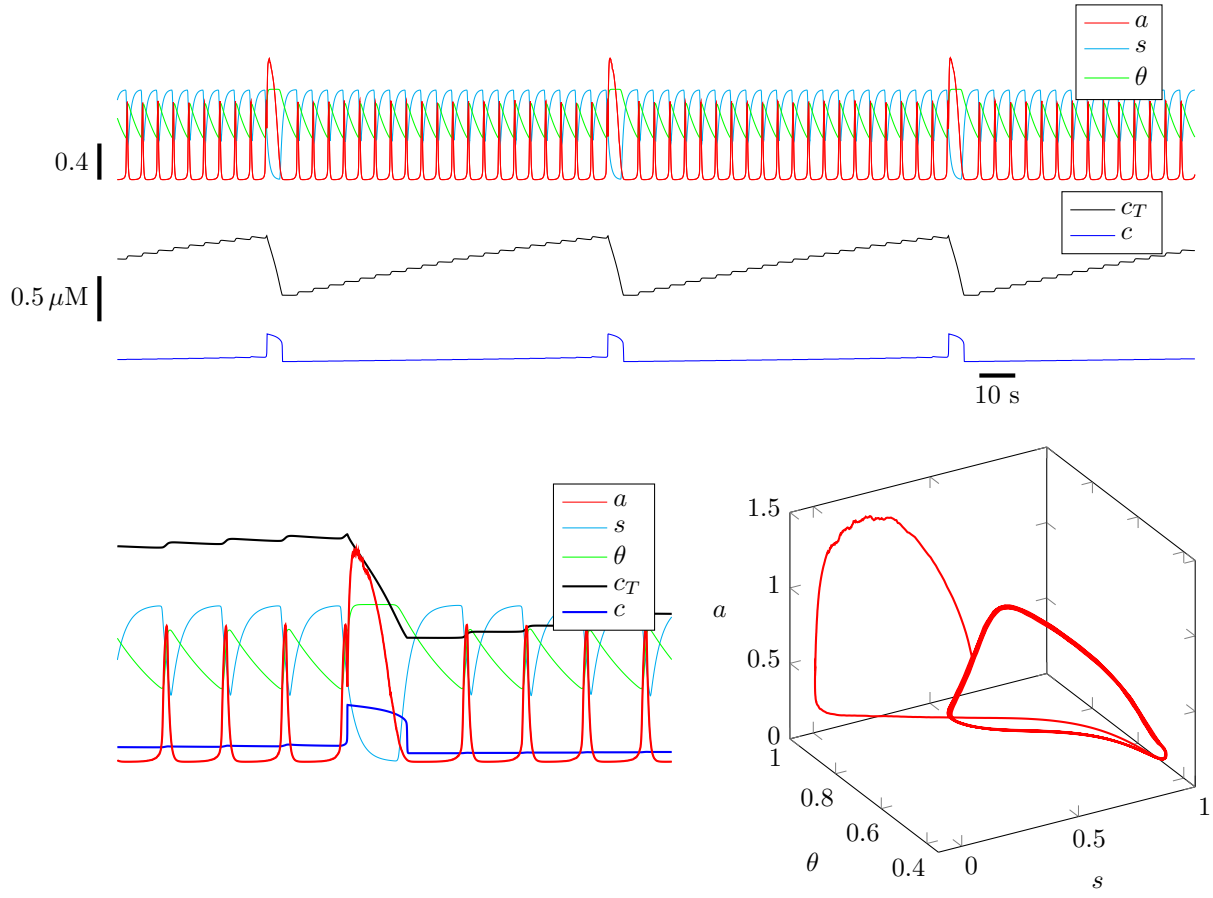

Figure 8: Model showing eupnea and sigh systems connected together. Top panel: solution of all five state variables. Left: A zoom in on the sigh event, building off the back of a eupnea breath. Right: phase diagram of the three eupnea sub-system state variables with a sigh included.